Supplementary material:

Table S1: Redox potentials ($E_{1/2}^0$) vs. Fc/Fc^+ for the redox transition $M^{IV} \leftrightarrow M^V$ measured with differential pulse voltammetry at 25°C in acetonitrile and referenced internally versus Fc/Fc^+ if not stated explicitly otherwise, the temperature dependences of the redox potentials (gradient) and the entropies (ΔS) for the reduction calculated from the latter; [a] calculated from referencing versus Ag/AgCl; [b] measurement in water; [c] measurement in dmf; [d] measured by cyclic voltammetry; [e] data from literature corrected by the T-dependence of the reference electrode[7], [f] investigated redox transition was $M^V \leftrightarrow M^{VI}$.

	$E_{1/2}^0$ [V]	gradient [mV/K]	ΔS [J/mol·K]
1a[b][d]	-0.26[a]	-1.41 ± 0.080	-136.04 ± 7.72
1b[b][d]	-0.59 [a]	-2.13 ± 0.049	-205.51 ± 4.73
2a[b]	-0.56[a]	-0.84 ± 0.111	-81.43 ± 10.71
2b[b]	-0.81[a]	-1.33 ± 0.069	-128.33 ± 6.66
3a	-0.80	0.46 ± 0.081	44.78 ± 7.79
3a[f]	-0.02	0.68 ± 0.061	65.24 ± 5.89
3b	-1.49	0.91 ± 0.072	87.35 ± 6.99
3b[f]	-0.61	1.33 ± 0.126	128.33 ± 12.13
4a	-0.77	0.05 ± 0.075	5.09 ± 7.22
4a[f]	-0.03	0.25 ± 0.115	24.27 ± 11.10
4b	-1.45	0.20 ± 0.118	19.19 ± 11.41
4b[f]	-0.75	0.41 ± 0.088	39.40 ± 8.49
5a[d]	0.00	-1.13 ± 0.106	-109.03 ± 10.20
5b[d]	-0.67	-1.27 ± 0.078	-122.54 ± 7.54
6a	-0.31	-0.33 ± 0.025	-32.03 ± 2.37
6b	-0.67	-1.79 ± 0.066	-172.71 ± 6.37
7a[d]	0.00	0.31 ± 0.060	29.50 ± 5.60
7b[d]	-0.07	0.79 ± 0.080	76.22 ± 7.72
7a[c][d]	0.04	0.28 ± 0.046	27.02 ± 4.45
7b[c][d]	-0.10	0.86 ± 0.133	83.26 ± 12.82
8a	-1.22	-0.73 ± 0.085	-70.85 ± 8.25
8b	-1.39	-1.01 ± 0.070	-97.45 ± 6.80
9a[e]	-0.78	0.059 ± 0.033	5.69 ± 3.18
9b[e]	-1.30	0.201 ± 0.094	19.39 ± 9.07
10a[e]	0.09	-1.256 ± 0.043	-121.19 ± 41.49

10b[e]	-0.09	-1.815 ± 0.102	-175.12 ± 9.84
11a[e]	-0.74	0.600 ± 0.344	57.89 ± 33.19
11b[e]	-1.33	0.689 ± 0.072	66.48 ± 6.95
12a[e]	-1.33	0.540 ± 0.131	52.10 ± 12.64
12b[e]	-1.36	0.991 ± 0.149	95.62 ± 14.38

Data and Graphs for the individual pairs

The voltammograms shown were subject to automatic baseline correction and/or smoothing where applicable.
For the linear regressions shown for each pair of newly investigated molybdenum and tungsten compounds the correlation coefficient (R) is defined as:

$$R = \frac{\sum_{i=1}^{n} \omega_i \cdot (x_i - \bar{x}) \cdot (y_i - \bar{y})}{\sqrt{\sum_{i=1}^{n} \omega_i \cdot (x_i - \bar{x})^2} \cdot \sqrt{\sum_{i=1}^{n} \omega_i \cdot (y_i \cdot \bar{y})^2}}$$

(with ω = weight and x_i,y_i = data points)

and the standard deviation (SD) of the linear regression is defined as:

$$SD = \sqrt{\sum_{i=1}^{N} \frac{(y_i - (A + B \cdot x_i))^2}{N - 2}}$$

(with A = interception with y-axis and B = gradient).

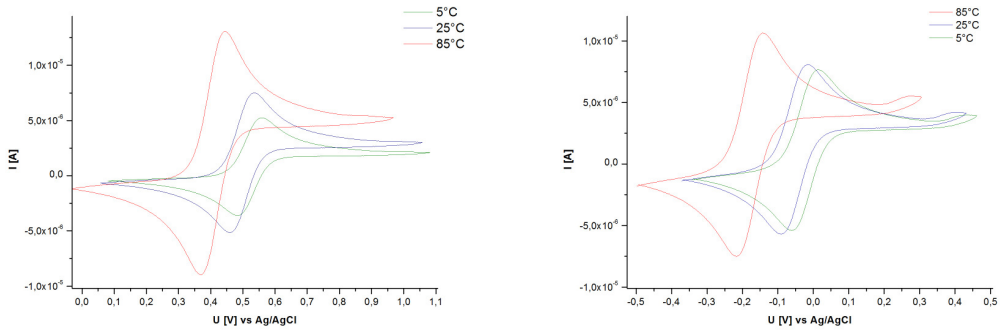

Figure S1**:** Cyclic voltammograms of $[MoO_2(CN)_4]^{4-}$ (left, **1a**) and $[WO_2(CN)_4]^{4-}$ (right, **1b**) at the highest, the lowest and at the reference temperature of 25°C.

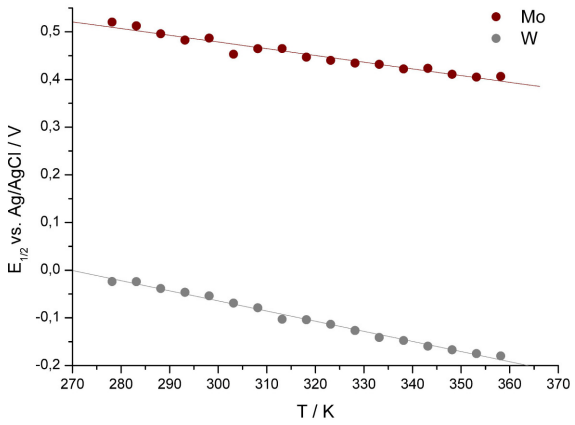

Figure S2**:** The redox potential's temperature dependence of the $[MO_2(CN)_4]^{4-}/[MO_2(CN)_4]^{3-}$ couples with linear fits. Mo: R = -0.976; SD = 0.00814; W: R = -0.996; SD = 0.00498

Table S2: Measured average redox potentials with standard error of the mean value (SEM) for the redox transition $M^{IV} \leftrightarrow M^{V}$ for **1a** $[MoO_2(CN)_4]^{4-}$ and **1b** $[WO_2(CN)_4]^{4-}$.

	1a $[MoO_2(CN)_4]^{4-}$		**1b $[WO_2(CN)_4]^{4-}$**	
T [K]	E [V]	SEM [V]	E [V]	SEM [V]
278.15	0.5204	0.0215	-0.0239	0.0098
283.15	0.5124	0.0242	-0.0241	0.0047
288.15	0.4957	0.0469	-0.0384	0.0105
293.15	0.4827	0.0353	-0.0465	0.0049
298.15	0.4868	0.0123	-0.0538	0.0105
303.15	0.4530	0.0466	-0.0689	0.0049
308.15	0.4646	0.0071	-0.0788	0.0049
313.15	0.4649	0.0167	-0.1030	0.0318
318.15	0.4468	0.0091	-0.1040	0.0050
323.15	0.4400	0.0206	-0.1136	0.0043
328.15	0.4343	0.0102	-0.1266	0.0040
333.15	0.4318	0.0186	-0.1412	0.0085
338.15	0.4221	0.0174	-0.1475	0.0045
343.15	0.4235	0.0193	-0.1594	0.0135
348.15	0.4109	0.0114	-0.1670	0.0079
353.15	0.4050	0.0179	-0.1750	0.0037
358.15	0.4064	0.0336	-0.1799	0.0046

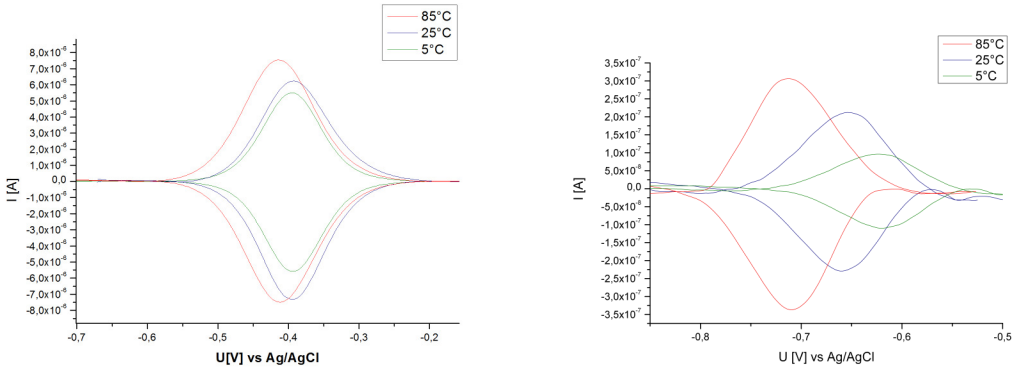

Figure S3**:** Differential pulse voltammograms of $[Mo(CN)_8]^{4-}$ (left, **2a**) and $[W(CN)_8]^{4-}$ (right, **2b**) at the highest, the lowest and at the reference temperature of 25°C.

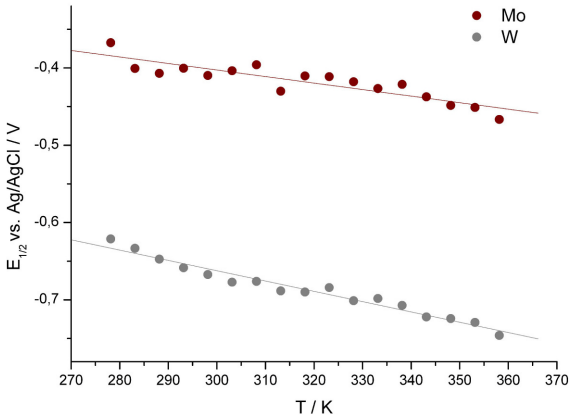

Figure S4**:** The redox potential's temperature dependence of the $[M(CN)_8]^{4-}/[M(CN)_8]^{3-}$ couples with linear fits. Mo: R = -0.891; SD = 0.01125; W: R = -0.980; SD = 0.00698

Table S3: Measured average redox potentials with standard error of the mean value (SEM) for the redox transition $M^{IV} \leftrightarrow M^{V}$ for **2a** $[Mo(CN)_8]^{4-}$ and **2b** $[W(CN)_8]^{4-}$.

	2a $[Mo(CN)_8]^{4-}$		2b $[W(CN)_8]^{4-}$	
T [K]	E [V]	SEM [V]	E [V]	SEM [V]
278.15	-0.3674	0.0133	-0.6212	0.0112
283.15	-0.4007	0.0157	-0.6333	0.0157
288.15	-0.4070	0.0142	-0.6474	0.0226
293.15	-0.4004	0.0184	-0.6585	0.0133
298.15	-0.4098	0.0233	-0.6673	0.0184
303.15	-0.4036	0.0211	-0.6771	0.0176
308.15	-0.3959	0.0129	-0.6762	0.0374
313.15	-0.4301	0.0156	-0.6884	0.0299
318.15	-0.4103	0.0139	-0.6899	0.0316
323.15	-0.4113	0.0153	-0.6841	0.0233
328.15	-0.4179	0.0145	-0.7011	0.0283
333.15	-0.4267	0.0128	-0.6982	0.0209
338.15	-0.4213	0.0144	-0.7072	0.0413
343.15	-0.4374	0.0122	-0.7221	0.0213
348.15	-0.4485	0.0132	-0.7242	0.0213
353.15	-0.4512	0.0133	-0.7292	0.0141
358.15	-0.4666	0.0144	-0.7461	0.0153

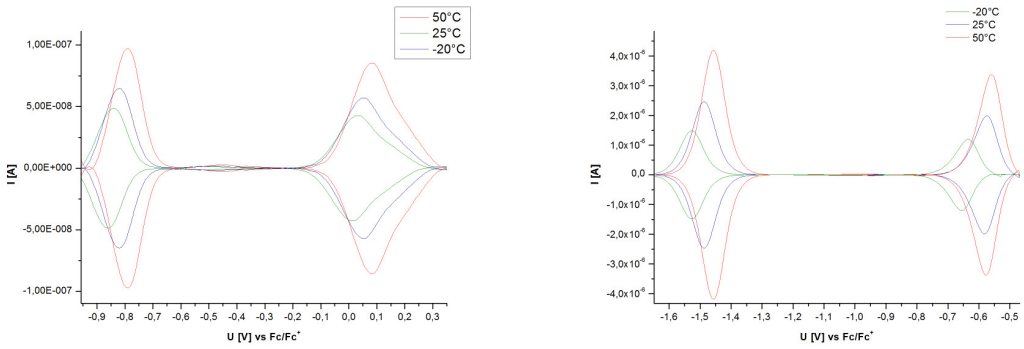

Figure S5**:** Differential pulse voltammograms for both redox processes $M^{IV} \leftrightarrow M^{V}$ and $M^{V} \leftrightarrow M^{VI}$ of $[MoO(tdt)_2]^{2-/-}$ (left, **3a**) and $[WO(tdt)_2]^{2-/-}$ (right, **3b**) at the highest, the lowest and at the reference temperature of 25°C.

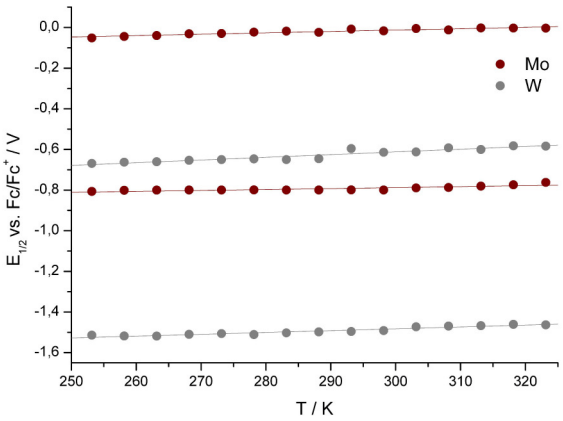

Figure S6**:** The redox potential's temperature dependence of the $[MO(tdt)_2]^{2-}/[MO(tdt)_2]^{-}$ and $[MO(tdt)_2]^{-}/[MO(tdt)_2]$ couples with linear fits. Mo: R = 0.847 and 0.951; SD = 0.00675 and 0.00511; W: R = 0.961 and 0.947; SD = 0.00606 and 0.01052

Table S4: Measured average redox potentials with standard error of the mean value (SEM) for both redox processes $M^{IV}\leftrightarrow M^{V}$ and $M^{V}\leftrightarrow M^{VI}$ for **3a** $[MoO(tdt)_2]^{2-/-/0}$ and **3b** $[WO(tdt)_2]^{2-/-/0}$. [a] Values for $M^{V}\leftrightarrow M^{VI}$.

	3a $[MoO(tdt)_2]^{2-}$		**3a**[a] $[MoO(tdt)_2]^{2-}$		**3b** $[WO(tdt)_2]^{-}$		**3b**[a] $[WO(tdt)_2]^{-}$	
T [K]	E [V]	SEM [V]	E [V]	SEM [V]	E [V]	SEM [V]	E [V]	SEM [V]
253.15	-0.8067	0.0185	-0.0516	0.0106	-1.5139	0.0205	-0.6689	0.0204
258.15	-0.8010	0.0091	-0.0447	0.0070	-1.5180	0.0156	-0.6630	0.0155
263.15	-0.8002	0.0070	-0.0397	0.0106	-1.5185	0.0156	-0.6610	0.0155
268.15	-0.7994	0.0084	-0.0313	0.0120	-1.5096	0.0248	-0.6536	0.0247
273.15	-0.7996	0.0063	-0.0294	0.0084	-1.5062	0.0304	-0.6502	0.0304
278.15	-0.7993	0.0091	-0.0229	0.0099	-1.5107	0.0248	-0.6462	0.0247
283.15	-0.7998	0.0128	-0.0185	0.0141	-1.5023	0.0262	-0.6498	0.0261
288.15	-0.7998	0.0117	-0.0240	0.0007	-1.4978	0.0686	-0.6453	0.0685
293.15	-0.7991	0.0141	-0.0081	0.0091	-1.4959	0.0342	-0.5959	0.0342
298.15	-0.7996	0.0127	-0.0167	0.0233	-1.4910	0.0288	-0.6139	0.0287
303.15	-0.7891	0.0127	-0.0052	0.0219	-1.4725	0.0629	-0.6125	0.0629
308.15	-0.7872	0.0120	-0.0123	0.0269	-1.4691	0.0615	-0.5921	0.0615
313.15	-0.7808	0.0127	-0.0023	0.0233	-1.4671	0.0226	-0.6001	0.0226
318.15	-0.7742	0.0127	-0.0029	0.0233	-1.4607	0.0141	-0.5822	0.0141
323.15	-0.7622	0.0217	-0.0034	0.0233	-1.4628	0.0132	-0.5838	0.0132

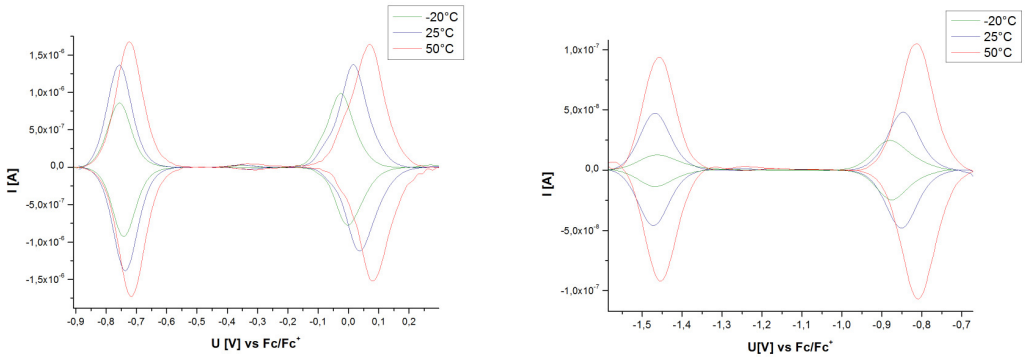

Figure S7**:** Differential pulse voltammograms for both redox processes $M^{IV} \leftrightarrow M^{V}$ and $M^{V} \leftrightarrow M^{VI}$ of $[MoO(vdt)_2]^{2-/-}$ (left, **4a**) and $[WO(vdt)_2]^{2-/-}$ (right, 4**b**) at the highest, the lowest and at the reference temperature of 25°C.

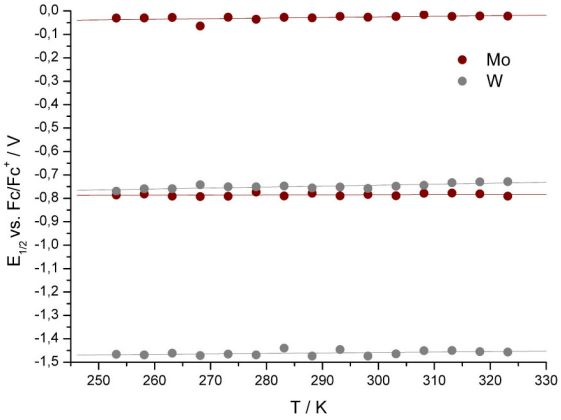

Figure S8**:** The redox potential's temperature dependence of the $[MO(vdt)_2]^{2-}/[MO(vdt)_2]^{-}$ and $[MO(vdt)_2]^{-}/[MO(vdt)_2]$ couples with linear fits. Mo: R = 0.192 and 0.519; SD = 0.00626 and 0.00962; W: R = 0.423 and 0.790; SD = 0.00989 and 0.00735

Table S5: Measured average redox potentials with standard error of the mean value (SEM) for both redox processes $M^{IV}\leftrightarrow M^{V}$ and $M^{V}\leftrightarrow M^{VI}$ for **4a** $[MoO(vdt)_2]^{2-/-/0}$ and **4b** $[WO(vdt)_2]^{2-/-/0}$. [a] Values for $M^{V}\leftrightarrow M^{VI}$.

	4a $[MoO(vdt)_2]^{2-}$		**4a**[a] $[MoO(vdt)_2]^{2-}$		**4b** $[WO(vdt)_2]^{2-}$		**4b**[a] $[WO(vdt)_2]^{2-}$	
T [K]	E [V]	SEM [V]	E [V]	SEM [V]	E [V]	SEM [V]	E [V]	SEM [V]
253.15	-0.7860	0.0062	-0.0304	0.0160	-1.4661	0.0391	-0.7699	0.0152
258.15	-0.7815	0.0061	-0.0297	0.0292	-1.4689	0.0292	-0.7592	0.0288
263.15	-0.7906	0.0065	-0.0276	0.0292	-1.4616	0.0298	-0.7588	0.0056
268.15	-0.7924	0.0061	-0.0660	0.0281	-1.4715	0.0284	-0.7423	0.0284
273.15	-0.7914	0.0011	-0.0267	0.0051	-1.4653	0.0292	-0.7507	0.0053
278.15	-0.7731	0.0012	-0.0355	0.0282	-1.4688	0.0292	-0.7508	0.0288
283.15	-0.7900	0.0023	-0.0273	0.0055	-1.4399	0.0281	-0.7472	0.0051
288.15	-0.7786	0.0296	-0.0294	0.0284	-1.4735	0.0282	-0.7557	0.0282
293.15	-0.7893	0.0502	-0.0234	0.0044	-1.4461	0.0261	-0.7518	0.0050
298.15	-0.7839	0.0282	-0.0266	0.0064	-1.4736	0.0282	-0.7581	0.0276
303.15	-0.7889	0.0291	-0.0238	0.0052	-1.4643	0.0282	-0.7481	0.0275
308.15	-0.7787	0.0291	-0.0161	0.0061	-1.4509	0.0271	-0.7444	0.0273
313.15	-0.7776	0.0285	-0.0232	0.0052	-1.4501	0.0282	-0.7333	0.0270
318.15	-0.7811	0.0292	-0.0216	0.0054	-1.4550	0.0271	-0.7297	0.0268
323.15	-0.7910	0.0061	-0.0219	0.0063	-1.4564	0.0291	-0.7289	0.0266

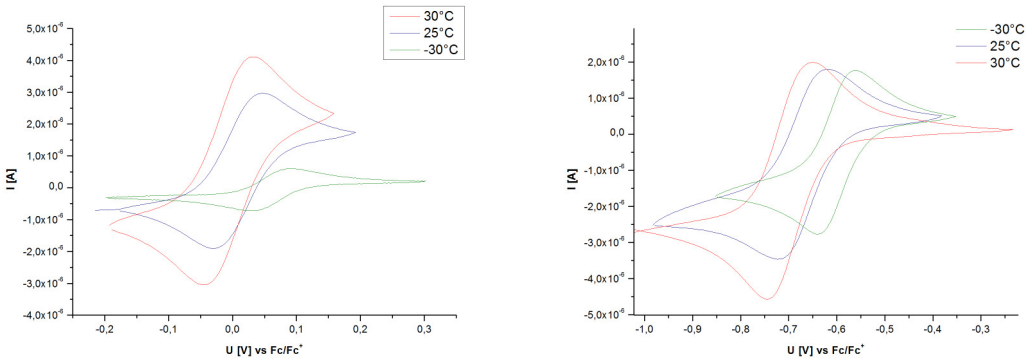

Figure S9**:** Cyclic voltammograms of $[MoCl_4(MeCN)_2]$ (left, **5a**) and $[WCl_4(MeCN)_2]$ (right, **5b**) at the highest, the lowest and at the reference temperature of 25°C.

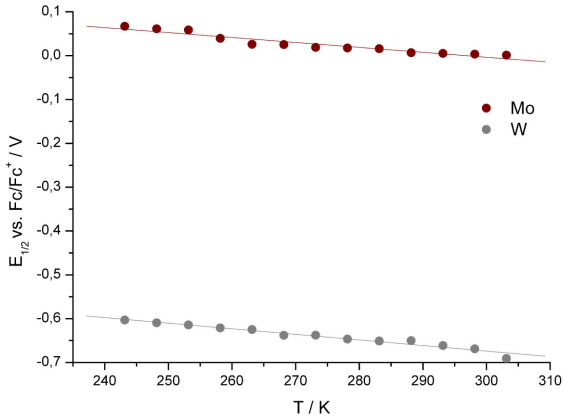

Figure S10**:** The redox potential's temperature dependence of the $[MCl_4(MeCN)_2]/[MCl_4(MeCN)_2]^+$ couples with linear fits. Mo: R = -0.955; SD = 0.00713; W: R = -0.980; SD = 0.00527

Table S6: Measured average redox potentials with standard error of the mean value (SEM) for the redox transition $M^{IV} \leftrightarrow M^{V}$ for **5a** $MoCl_4(MeCN)_2$ and **5b** $WCl_4(MeCN)_2$.

	5a $MoCl_4(MeCN)_2$		**5b** $WCl_4(MeCN)_2$	
T [K]	E [V]	SEM [V]	E [V]	SEM [V]
243.15	0.06732	0.02479	-0.60310	0.02831
248.15	0.06129	0.02612	-0.60942	0.02832
253.15	0.05875	0.02656	-0.61442	0.02859
258.15	0.03954	0.02722	-0.62119	0.02891
263.15	0.02605	0.01955	-0.62480	0.02913
268.15	0.02540	0.01951	-0.63795	0.02832
273.15	0.01896	0.01985	-0.63774	0.02979
278.15	0.01766	0.01996	-0.64667	0.02859
283.15	0.01597	0.02002	-0.65107	0.02995
288.15	0.00679	0.01958	-0.65010	0.02863
293.15	0.00529	0.01953	-0.66136	0.02909
298.15	0.00351	0.01983	-0.66877	0.02989
303.15	0.00113	0.03054	-0.69096	0.02890

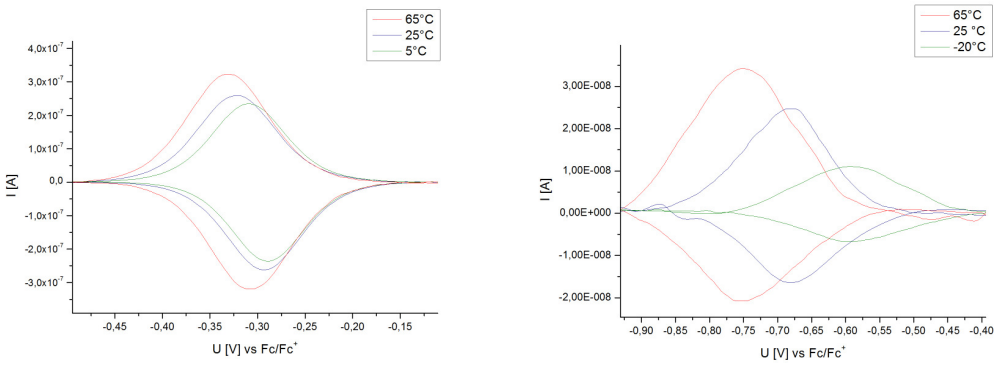

Figure S11**:** Differential pulse voltammograms of $[MoO(qdt)_2]^{2-}$ (left, **6a**) and $[WO(qdt)_2]^{2-}$ (right, **6b**) at the highest, the lowest and at the reference temperature of 25°C.

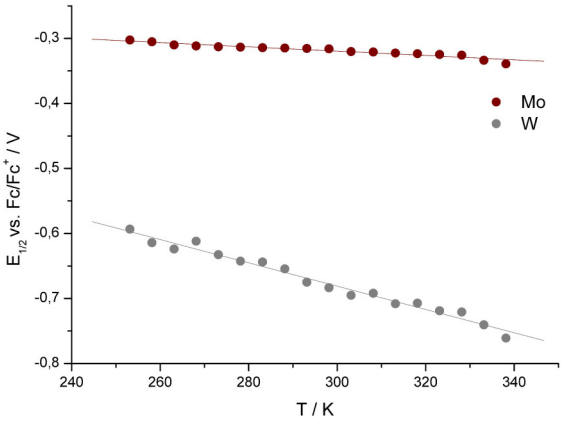

Figure S12**:** The redox potential's temperature dependence of the $[MO(qdt)_2]^{2-}/[MO(qdt)_2]^{1-}$ couples with linear fits. Mo: R = -0.959; SD = 0.00271; W: R = -0.989; SD = 0.00727

Table S7: Measured average redox potentials with standard error of the mean value (SEM) for the redox transition $M^{IV} \leftrightarrow M^{V}$ for **6a** $[MoO(qdt)_2]^{2-}$ and **6b** $[WO(qdt)_2]^{2-}$.

	6a $[MoO(qdt)_2]^{2-}$		**6b** $[WO(qdt)_2]^{2-}$	
T [K]	E [V]	SEM [V]	E [V]	SEM [V]
253.15	-0.30241	0.03674	-0.59333	0.01787
258.15	-0.30517	0.02177	-0.61415	0.04245
263.15	-0.31003	0.03679	-0.62395	0.01923
268.15	-0.31169	0.03748	-0.61191	0.01322
273.15	-0.31286	0.03939	-0.63258	0.02313
278.15	-0.31349	0.02942	-0.64255	0.04521
283.15	-0.31433	0.03173	-0.64392	0.01773
288.15	-0.31491	0.03133	-0.65456	0.02714
293.15	-0.31548	0.03674	-0.67504	0.01985
298.15	-0.31614	0.05177	-0.68348	0.01287
303.15	-0.32033	0.03679	-0.69504	0.03937
308.15	-0.32100	0.07748	-0.69210	0.03519
313.15	-0.32257	0.03939	-0.70806	0.00750
318.15	-0.32353	0.08139	-0.70731	0.02577
323.15	-0.32467	0.03679	-0.71887	0.04223
328.15	-0.32574	0.05947	-0.72082	0.04342
333.15	-0.33361	0.04475	-0.74041	0.03073
338.15	-0.33916	0.06064	-0.76086	0.00292

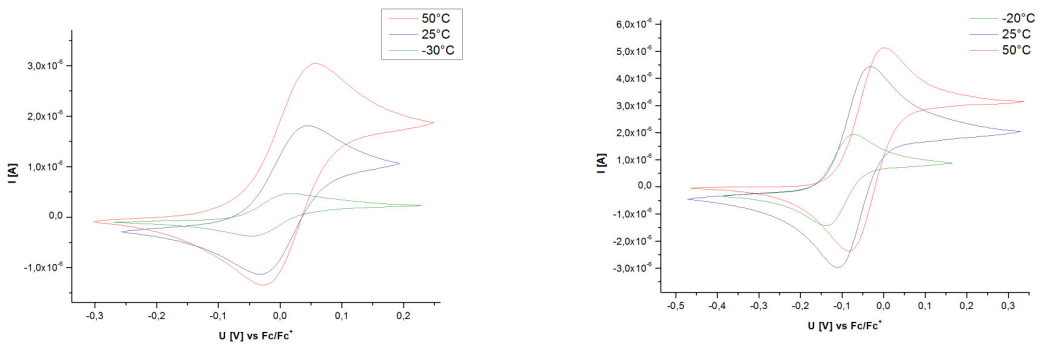

Figure S13**:** Cyclic voltammograms of $[MoCp_2Cl_2]$ in CH_3CN (left, **7a**) and $[WCp_2Cl_2]$ in CH_3CN (right, **7b**) at the highest, the lowest and at the reference temperature of 25°C.

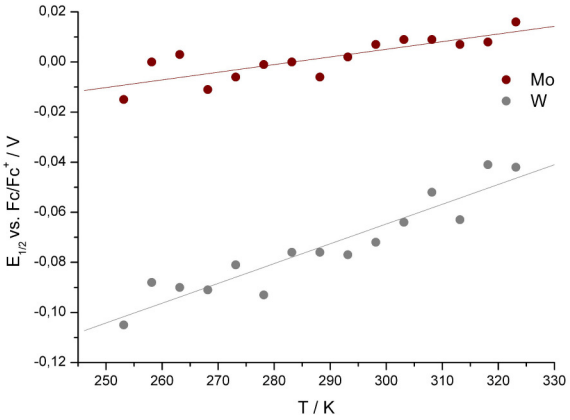

Figure S14**:** The redox potential's temperature dependence of the $[MoCp_2Cl_2]/[MoCp_2Cl_2]^+$ couples in CH_3CN with linear fits. *Mo: R* = 0.817*; SD* = 0.00500*; W: R* = 0.939*; SD* = 0.00669

Table S8: Measured average redox potentials with standard error of the mean value (SEM) for the redox transition $M^{IV} \leftrightarrow M^{V}$ for **7a** $MoCp_2Cl_2$ in CH_3CN and **7b** WCp_2Cl_2 in CH_3CN.

	7a $MoCp_2Cl_2$		**7b** WCp_2Cl_2	
T [K]	E [V]	SEM [V]	E [V]	SEM [V]
253.15	-0.015	0.01349	-0.105	0.01523
258.15	0.000	0.01349	-0.088	0.01433
263.15	0.003	0.01295	-0.090	0.01628
268.15	-0.011	0.00996	-0.091	0.00466
273.15	-0.006	0.01241	-0.081	0.01524
278.15	-0.001	0.00239	-0.093	0.01903
283.15	0.000	0.01187	-0.076	0.01623
288.15	-0.006	0.01349	-0.076	0.01657
293.15	0.002	0.01187	-0.077	0.01634
298.15	0.007	0.01975	-0.072	0.03847
303.15	0.009	0.01147	-0.064	0.01515
308.15	0.009	0.01295	-0.052	0.01594
313.15	0.007	0.02187	-0.063	0.01664
318.15	0.008	0.03241	-0.041	0.01439
323.15	0.016	0.04187	-0.042	0.02544

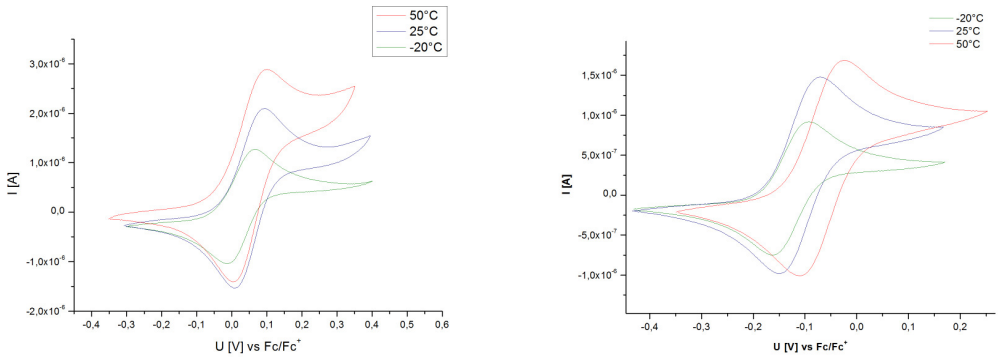

Figure S15**:** Cyclic voltammograms of [$MoCp_2Cl_2$] in dmf (left, **7a**) and [WCp_2Cl_2] in dmf (right, 7**b**) at the highest, the lowest and at the reference temperature of 25°C.

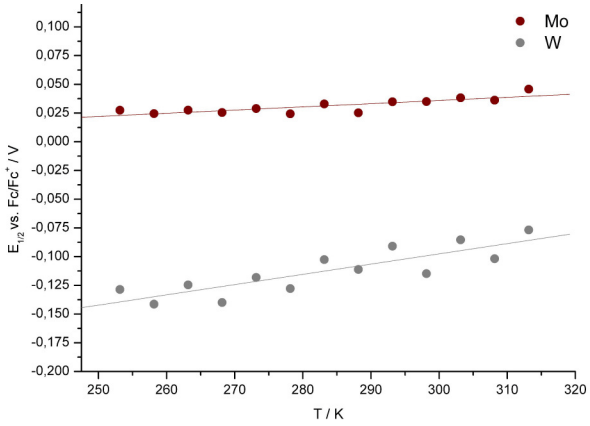

Figure S16**:** The redox potential's temperature dependence of the [$MoCp_2Cl_2$]/[$MoCp_2Cl_2$]$^+$ couples in dmf with linear fits. Mo: R = 0.828; SD = 0.00383; W: R = 0.85493; SD = 0.01101

Table S9: Measured average redox potentials with standard error of the mean value (SEM) for the redox transition $M^{IV} \leftrightarrow M^{V}$ for **7a** $MoCp_2Cl_2$ and **7b** WCp_2Cl_2 in dmf.

	7a $MoCp_2Cl_2$		**7b** WCp_2Cl_2	
T [K]	E [V]	SEM [V]	E [V]	SEM [V]
253.15	0.0274	0.0187	-0.1286	0.0196
258.15	0.0245	0.0186	-0.1313	0.0151
263.15	0.0275	0.0186	-0.1246	0.0153
268.15	0.0254	0.0179	-0.1299	0.0165
273.15	0.0289	0.0172	-0.1184	0.0151
278.15	0.0243	0.0179	-0.1278	0.0152
283.15	0.0328	0.0188	-0.1025	0.0158
288.15	0.0252	0.0179	-0.1111	0.0165
293.15	0.0348	0.0186	-0.1108	0.0158
298.15	0.0349	0.0179	-0.1148	0.0117
303.15	0.0383	0.0187	-0.1053	0.0165
308.15	0.0361	0.0189	-0.0818	0.0151
313.15	0.0458	0.0186	-0.0768	0.0165
318.15	0.0464	0.0194	-0.0686	0.0179
323.15	0.0475	0.0171	-0.0513	0.0194

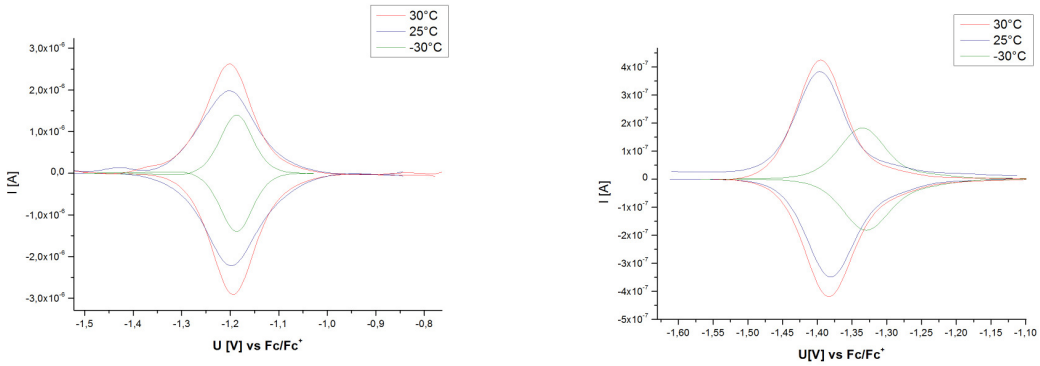

Figure S17**:** Differential pulse voltammograms of $[MoO(SPh)_4]^-$ (left, **8a**) and $[WO(SPh)_4]^-$ (right, **8b**) at the highest, the lowest and at the reference temperature of 25°C.

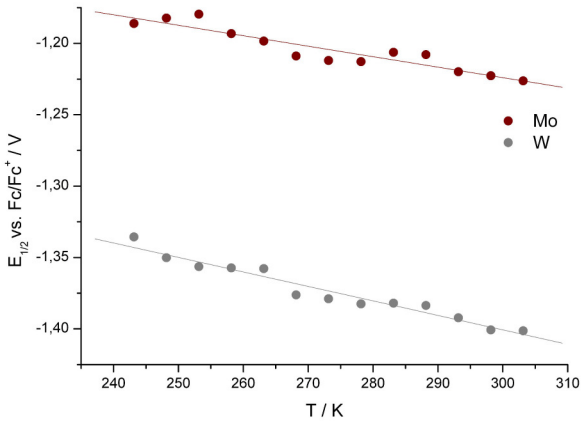

Figure S18**:** The redox potential's temperature dependence of the $[MO(SPh)_4]^-$/$[MO(SPh)_4]$ couples with linear fits. *Mo: R* = -0.*933; SD* = 0.00*577; W: R* = -0.*974; SD* = 0.00*475*

Table S10: Measured average redox potentials with standard error of the mean value (SEM) for the redox transition $M^{IV} \leftrightarrow M^{V}$ for **8a** $[MoO(SPh)_4]^-$ and **8b** $[WO(SPh)_4]^-$.

	8a $[MoO(SPh)_4]^-$		**8b** $[WO(SPh)_4]^-$	
T [K]	E [V]	SEM [V]	E [V]	SEM [V]
243.15	-1.1861	0.0057	-1.3356	0.0309
248.15	-1.1823	0.0009	-1.3502	0.0219
253.15	-1.1796	0.0045	-1.3564	0.0308
258.15	-1.1932	0.0029	-1.3573	0.0162
263.15	-1.1984	0.0134	-1.3578	0.0289
268.15	-1.2089	0.0115	-1.3762	0.0014
273.15	-1.2120	0.0113	-1.3789	0.0183
278.15	-1.2128	0.0133	-1.3825	0.0162
283.15	-1.2063	0.0099	-1.3820	0.0183
288.15	-1.2079	0.0059	-1.3836	0.0162
293.15	-1.2199	0.0077	-1.3922	0.0162
298.15	-1.2227	0.0205	-1.4007	0.0271
303.15	-1.2263	0.0205	-1.4013	0.0271